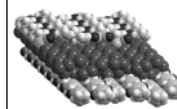


# New developments in the chemistry of organoantimony and -bismuth rings



CSR

Hans Joachim Breunig<sup>\*a</sup> and Roland Rösler<sup>b</sup>

<sup>a</sup> Institut für Anorganische und Physikalische Chemie, Fachbereich 2, Universität Bremen, Postfach 330440, D-28334 Bremen, Germany. E-mail: breunig@chemie.uni-bremen.de

<sup>b</sup> Chemistry Department, Dalhousie University, Halifax, Nova Scotia, Canada B3H 4J3

Received 3rd May 2000

First published as an Advance Article on the web 28th September 2000

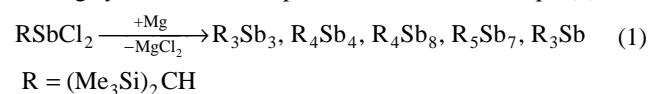
Novel organoantimony homocycles comprise a three-membered antimony ring,  $R_3Sb_3$ , organoantimony polycycles,  $R_4Sb_8$ ,  $R_5Sb_7$ , and transition metal carbonyl complexes with the *t*-Bu<sub>4</sub>Sb<sub>4</sub> or *t*-Bu<sub>3</sub>Sb<sub>4</sub> ligand. In this review the use of *t*-Bu<sub>4</sub>Sb<sub>4</sub> as a source for complexes with the Sb<sub>2</sub> or *cyclo*-Sb<sub>3</sub> ligands and the synthesis and characterisation of the first organobismuth monocycles,  $R_nBi_n$  ( $n = 3, 4$ ) are also discussed.

## 1 Introduction

The study of the chemistry of organoantimony oligomers,  $R_nSb_n$ , over the last decades has revealed an extraordinary diversity of cyclic and noncyclic systems under a strong influence of the organic substituents: non-bulky substituents ( $R = Me, Et, Pr, Ph, Tol, etc.$ ) give rise to highly flexible antimony homocycles with equilibria between rings of different size or polymers. In the gas phase there are trimeric species, but in solution the most abundant oligomers are usually five-membered rings.<sup>1</sup> Cyclic hexamers,  $R_6Sb_6$  ( $R = Ph, Tol$ ) exist in crystalline phases.<sup>1</sup> Bulky groups ( $R = t-Bu, Mes, Cp^*, (Me_3Si)_2CH$ ) protect four-membered rings,  $R_4Sb_4$ , which preserve the ring size on phase transitions. Dimers,  $R_2Sb_2$  are also known. They exist with sterically overcrowded aryl groups ( $R = 2,4,6-[(Me_3Si)_2CH]_3C_6H_2, 2,6-Mes_2C_6H_3, etc.$ ). The chemistry of the organoantimony and -bismuth dimers has been discussed in an excellent review that appeared in 1999.<sup>2</sup> In this present article, developments in the field of organoantimony homocycles and their bismuth analogues are reported.

## 2 Syntheses and reactions of organoantimony and -bismuth homocycles: $R_3Sb_3, R_4Sb_4, R_4Sb_8, R_5Sb_7; R_3Bi_3, R_4Bi_4$ ( $R = (Me_3Si)_2CH$ )

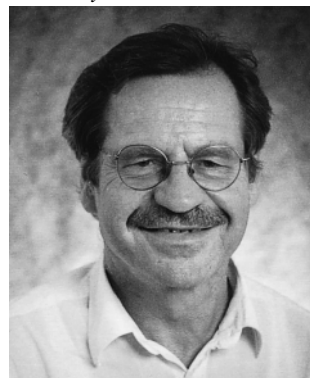
The most versatile organic group for the protection of antimony or bismuth homocycles proved to be the bis(trimethylsilyl)methyl substituent. Due to the unsymmetrical shape and the absence of  $\beta$ -hydrogen atoms it combines effective steric protection in the periphery of the cyclic species with relatively little sterical hindrance between adjacent *cis*-substituents and stability towards  $\beta$ -elimination. With  $RECl_2$  ( $E = Sb, Bi; R = (Me_3Si)_2CH$ ), easily accessible starting materials for ring syntheses are available.<sup>3,4</sup> When  $RSbCl_2$  is reacted with magnesium in tetrahydrofuran, following a standard procedure for ring synthesis, various products are obtained [eqn. (1)].<sup>5,6</sup>



The main product, the four-membered ring  $R_4Sb_4$  ( $R = (Me_3Si)_2CH$ ) is formed in about 50% yield. It crystallises from a petroleum ether solution of the product mixture. Using chromatography the polycyclic compounds  $R_7Sb_5$  and  $R_4Sb_8$  are isolated as orange crystals. The trimer  $R_3Sb_3$  and the trialkylantimony compound  $R_3Sb$  remain as mixtures.

The formation of the monocycles  $R_3Sb_3$  and  $R_4Sb_4$  results from a relatively simple dehalogenation process, which presumably proceeds stepwise through Grignard-like monomeric or oligomeric intermediates of the type  $Cl-Mg-(Sb(R))_n-Cl$  ( $n = 1-4$ ). The reactions leading to the polycycles are more diverse. They represent the first steps of a general reaction path

Hans Joachim Breunig was born in 1945 in Blochwitz, Germany and studied chemistry at the University of Würzburg.



Hans Joachim Breunig

He received his PhD from the Technical University Berlin, working in the group of Professor Herbert Schumann, and in 1975 moved to the University of Bremen, where he is now Professor of Inorganic Chemistry. His research interests focus upon the syntheses and properties of organometallic compounds of antimony and bismuth with element–element bonds.

Roland Rösler was born in Petrosani, Romania, in 1971. He studied chemistry at the Babes–Bolyai University in Cluj

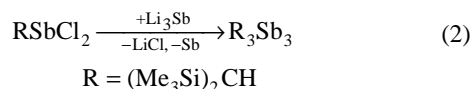


Roland Rösler

Napoca, Romania. Subsequently he moved to the University of Bremen, Germany where he received his PhD, working in the group of Professor Hans J. Breunig. Since 1999 he has been a postdoctoral fellow at Dalhousie University, Halifax, Canada, working in the group of Professor Neil Burford in the field of low coordinated antimony and bismuth compounds.

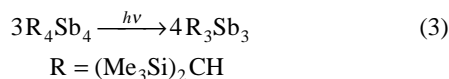
for organometallic compounds with element–element bonds, *i.e.* the migration of the organic substituents and the formation of mononuclear metal alkyls and elemental metal. However, these reactions are not trivial and attempts to isolate polycycles after the thermal decomposition of  $R_4Sb_4$  or  $R_3Sb_3$  were not successful. It is likely that the formation of the polycycles occurs during the reduction process [eqn. (1)].

Recently, several ways to increase the selectivity of the reduction [eqn. (1)] have been investigated. When a 4:1 molar mixture of  $RSbCl_2$  and  $SbCl_3$  is reduced with magnesium in tetrahydrofuran, instead of an increase of the fraction of polycycles a more efficient synthesis of the four-membered ring is achieved. A selective synthesis of the three-membered ring and not formation of polycycles is the result of the reduction of  $RSbCl_2$  with  $Li_3Sb$  in tetrahydrofuran at  $-70^\circ C$  [eqn. (2)].<sup>6</sup>

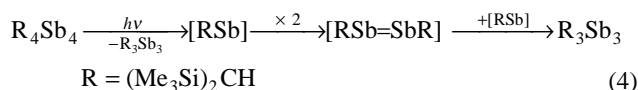


With this method the three-membered ring is obtained in 58% yield as a yellow oil with little tendency to crystallisation. Single crystals grow from a supersaturated solution in petroleum ether after inoculation with polycrystalline material.

Another way to prepare the three-membered ring is the photochemical ring contraction of the four-membered ring [eqn. (3)].<sup>6</sup>

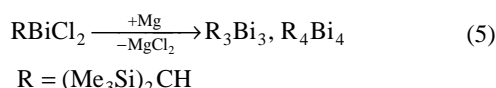


This photochemical reaction proceeds when a solution of  $R_4Sb_4$  in benzene is exposed to daylight for several months or to the light of a UV lamp for several minutes. Photochemical ring contraction reactions are well known in the chemistry of organosilicon homocycles<sup>7</sup> but they are novel in the field of *cyclo*-stibanes. A probable mechanism for the photochemical ring contraction might imply the formation of a stibinidene and a distibene as intermediates [eqn. (4)].

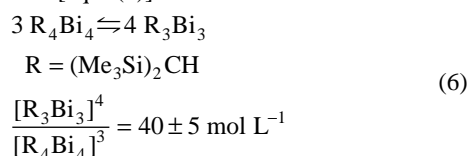


However, only very little is known about the photochemistry of *cyclo*-stibanes or other compounds with Sb–Sb bonds and other mechanisms including the formation of open chain biradicals might be equally effective. In view of the reversibility of all other ring–ring reactions in *cyclo*-stibane chemistry it is surprising that the photochemical formation of the trimer is not reversible. A possible explanation might be based on the hypsochromic shift in the absorption ranges between the tetramer and the trimer. The conjugation of the Sb–Sb  $\sigma$ -bonds, and as a consequence also the photochemical reactivity, should increase with the number of Sb–Sb bonds. This effect might drive the reaction towards the smaller antimony ring, which is less susceptible to the influence of light.

No polycycles, but three- and four-membered rings are formed when  $RBiCl_2$  reacts with magnesium in THF [eqn. (5)].<sup>8</sup>



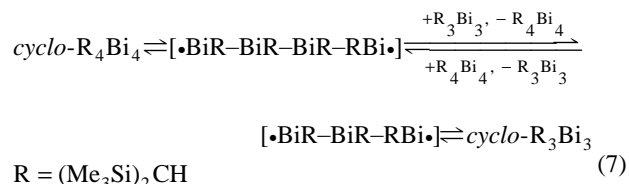
In contrast to the analogous antimony system, however, the bismuth rings interchange easily under thermal conditions in a ring–ring equilibrium [eqn. (6)].



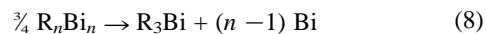
The equilibrium constant was measured in benzene at  $23^\circ C$ . According to the principle of Le Chatelier, the formation of the tetramer is favoured with higher concentrations and therefore the four-membered ring and not the trimer precipitates from the equilibrium mixture at low temperatures.

Fascinating colour effects are displayed by the bismuth ring system. The tetramer is black in the crystalline state, but green in solution in benzene. The colour of the trimer in solution is red. When benzene is added to the black crystals at low temperature, the four-membered ring compound dissolves to give a green colour. After several minutes the equilibrium is established and the red trimer becomes the most abundant species in the solution. When the red solution is cooled, under the influence of the entropy the equilibrium is shifted towards the tetramer and the solution becomes brown.

The mechanism of the reaction between the bismuth rings is not known. For thermal equilibria between *cyclo*-stibanes<sup>1</sup> a concerted mechanism with migrations of element–element  $\sigma$ -bonds has been proposed. In view of the steric protection of  $R_3Bi_3$  and  $R_4Bi_4$  through the bulky substituents it is unlikely that such a mechanism would work with bismuth. Instead, the fission of the relatively weak Bi–Bi bonds and the formation of biradical chains [eqn. (7)] is more likely. The formation of dimers  $R_2Bi_2$ , or monomers  $RBi$  is also possible. More research is required to establish a mechanism.



Biradical intermediates might also play a role in the observed decomposition reactions of the bismuth rings [eqn. (8)].



$n = 3, 4$ ;  $R = (Me_3Si)_2CH$

At  $23^\circ C$  in benzene the decomposition follows first-order kinetics. The concentrations decrease with  $\tau_{1/2}(R_4Bi_4) = 20.2 \pm 2.0$  h and  $\tau_{(1/2)R_3Bi_3} = 31.6 \pm 2.7$  h.

### 3 Structures of $R_3Sb_3$ , $R_3Bi_3$ , $R_4Sb_4$ , and $R_4Bi_4$ ( $R = (Me_3Si)_2CH$ )

The crystal structure of  $R_3Sb_3$  ( $R = (Me_3Si)_2CH$ ) as determined by X-ray crystallography<sup>6</sup> is depicted in Fig. 1. The  $R_3Sb_3$  molecules have a *cis*–*trans* configuration. A selection of geometric parameters is given in Table 1. The central core is an almost equilateral triangle of antimony atoms. The Sb–Sb bond lengths lie in the normal range for Sb–Sb single bonds. The sterically hindered situation of the *cis* substituents compared to the *trans* substituents is reflected in the C–Sb–Sb angles which are significantly wider between the *cis* groups. All the trimethylsilyl groups are directed towards the periphery of the ring.

In solution the *cis*–*trans* configuration of  $R_3Sb_3$  is also preserved. The  $^1H$  NMR spectra (Fig. 2) in  $C_6D_6$  contain three singlet signals of equal intensity for the methyl groups. Two signals stem from the pairs of diastereotopic  $Me_3Si$  groups of the alkyl substituents in *cis* positions. The third signals stems from the alkyl group in the *trans* position. The signals for the CH group appear in the correct 1:2 ratio of intensities between each other. There is a strong high-field shift for the methine protons at the substituents in *trans* positions. Mass spectra show the molecular ion of the trimer.

The analogous  $R_3Bi_3$  ring could not be characterised by crystallography because it is transformed into the tetramer on

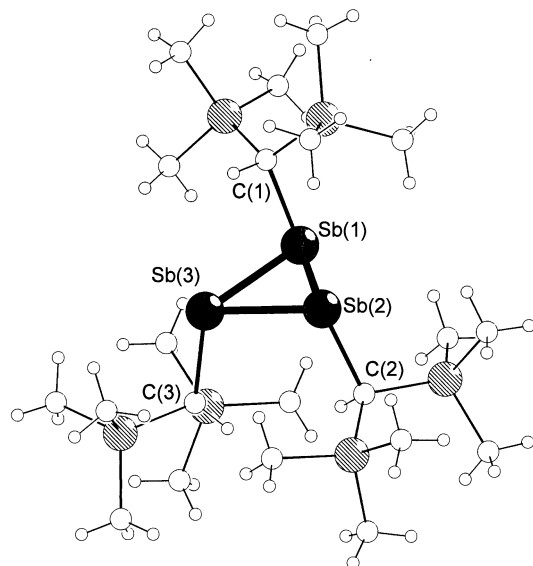


Fig. 1 Crystal structure of  $R_3Sb_3$  ( $R = (Me_3Si)_2CH$ ).

crystallisation. In solution, however, the structure could be determined through NMR spectroscopy. The  $^1H$  spectra of the equilibrium mixture with the trimer as most abundant species are shown in Fig. 2. The number and the relative intensities of signals for the bismuth trimer are similar to the signals of the antimony analogue and prove the identity of the three-membered bismuth ring in the *cis-trans* configuration.

Both four-membered rings,  $R_4Sb_4$  and  $R_4Bi_4$  ( $R = (Me_3Si)_2CH$ ), have been characterised by X-ray crystallography. The molecular structures are isotypal. The structure of the four-membered ring  $R_4Bi_4$  is depicted in Fig. 3. Selected geometric parameters for both  $R_4Sb_4$  and  $R_4Bi_4$  are presented in Table 1. The bond lengths are normal for single bonds between the elements. Under the influence of the sterical strain between the bulky alkyl substituents the element–element distances inside the central ring alternate between longer and shorter bond lengths and there is a wide range of E–E–C bond angles. It is not surprising that the detailed inspection of the geometric parameters reveals a sterically less congested situation in the case of the bismuth ring. The rings are considerably folded and it is remarkable that the fold angles are smaller for  $R_4Bi_4$  ( $112.6, 112.9^\circ$ ) than for  $R_4Sb_4$  ( $115.3, 115.5^\circ$ ).

It is generally accepted that the reason for the folding of the rings is to avoid eclipsed conformations of the bonds in the ring and to reduce steric interactions of the substituents in the 1,3-positions. In view of the relatively long Bi–Bi bonds it is expected that the repulsive forces should be smaller for the bismuth ring than for the antimony ring. However, a lower degree of hybridisation due to relativistic effects might result in smaller inter-ligand angles and might lead to an increase of steric repulsion between the ligands in the bismuth ring. Possibly not only repulsive but also attractive interactions should be considered. Attractive *trans*-annular interactions under the influence of dispersion (London) forces should be more pronounced for bismuth(i) than for antimony(i) and the relatively strong folding of the bismuth ring might be rather a consequence of attractive rather than repulsive force.

Table 1 Selected bond lengths and angles of  $R_3Sb_3$ ,  $R_4Sb_4$ ,  $R_4Sb_8$ , and  $R_4Bi_4$  ( $R = (Me_3Si)_2CH$ )

Compound	Sb–Sb or Bi–Bi/pm	Sb–C or Bi–C/pm	Sb–Sb–Sb or Bi–Bi–Bi/ $^\circ$	Sb–Sb–C or Bi–Bi–C/ $^\circ$	Ref.
$R_3Sb_3$	281.88(6)–284.53(6)	220.1(5)–221.0(5)	59.54(1)–60.47(1)	<i>cis</i> : 101.7(1)–111.3(1) <i>trans</i> : 90.0(1), 97.0(1)	6
$R_4Sb_4$	282.2(1)–287.8(1)	222.6(5)–223.2(4)	80.14(2)–80.75(1)	96.7(1)–110.6(1)	9
$R_4Sb_8$	278.4(4)–286.1(4)	215(3)–224(4)	84.7(1)–109.7(1)	96.2(8)–113.2(7)	5
$R_4Bi_4$	297.0(5)–304.4(2)	232(2)–239(2)	78.97(8)–79.93(6)	93.9(6)–109.5(5)	8

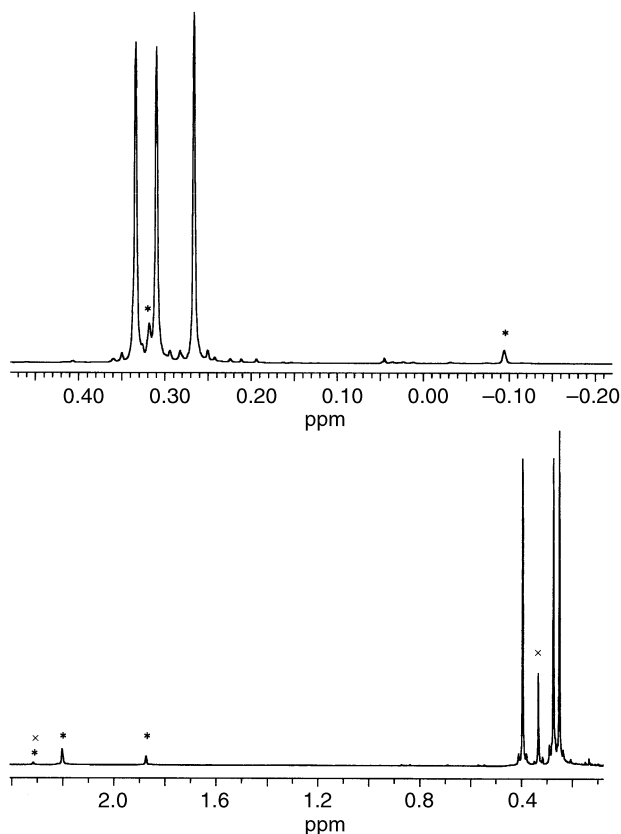


Fig. 2  $^1H$  NMR spectra of  $R_3Sb_3$  (above),  $R_3Bi_3$  and  $R_4Bi_4$  equilibrium mixture (below); \* indicates the signals corresponding to the methine protons,  $\times$  the signals due to the  $R_4Bi_4$  species.

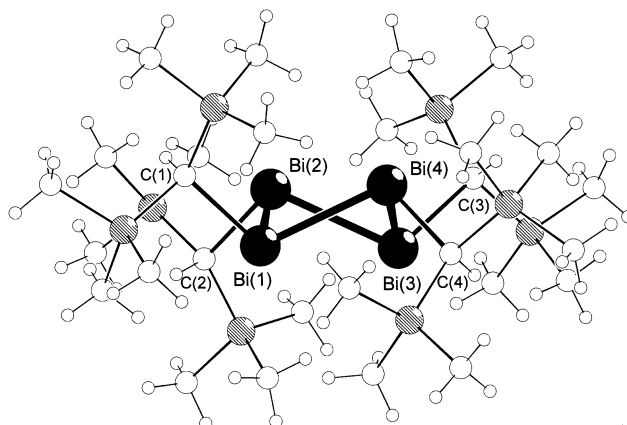


Fig. 3 Crystal structure of  $R_4Bi_4$  ( $R = (Me_3Si)_2CH$ ).

The main features of the ring structures of  $R_4Sb_4$  and  $R_4Bi_4$  are also preserved in solution. As expected for four-membered cycles with all-*trans* substituents, there is evidence from the  $^1H$  and  $^{13}C$  NMR spectra that all the substituents are equivalent and singlet signals are observed for the methyl and methine protons and for the carbon atoms respectively. Mass spectra were obtained for  $R_4Sb_4$  only. They show the identity of this ring also in the gas phase. Mass spectra of bismuth rings could not be obtained. Instead decomposition was observed.

## 4 Structures of R<sub>4</sub>Sb<sub>8</sub> and R<sub>5</sub>Sb<sub>7</sub>

Of the two polycycles only the structure of R<sub>4</sub>Sb<sub>8</sub> was determined by X-ray methods.<sup>5</sup> The molecular structure is depicted in Fig. 4. The core of the molecule is a tricyclic Sb<sub>8</sub> cage built of five-membered antimony rings in the envelope conformation, sharing common edges.

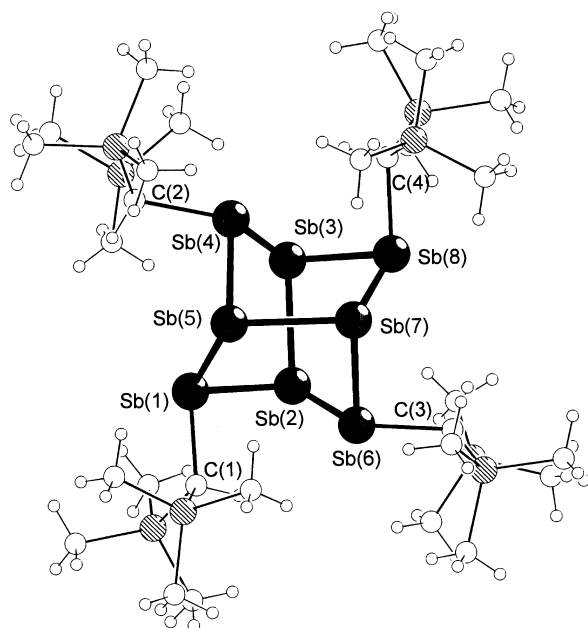


Fig. 4 Crystal structure of R<sub>4</sub>Sb<sub>8</sub> (R = (Me<sub>3</sub>Si)<sub>2</sub>CH).

The molecule is derived from a tetrahedron of four antimony atoms where RSb units are inserted in four of the six Sb–Sb bonds. The bond lengths and the bond angles (Table 1) vary across a relatively large range. Although no analogous clusters have been characterised by crystallography the motif of the cage is well known. It appears for instance as a section of the structure of Hittorf's phosphorus or in the mineral realgar, As<sub>4</sub>S<sub>4</sub>.

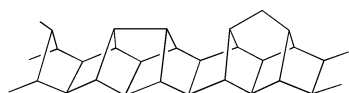


Fig. 5 Schematic structure of Hittorf's violet phosphorus.

The second polycycle, R<sub>5</sub>Sb<sub>7</sub> was characterised by mass spectrometry. By comparison with the structure of analogous phosphorus compounds<sup>10</sup> a bicyclic norbornane structure corresponding to a P<sub>7</sub> fragment of Hittorf's phosphorus is probable.

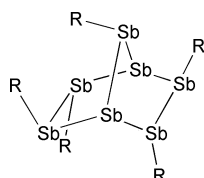


Fig. 6 Probable structure of R<sub>5</sub>Sb<sub>7</sub> (R = (Me<sub>3</sub>Si)<sub>2</sub>CH).

## 5 The role of *t*-Bu<sub>4</sub>Sb<sub>4</sub> in coordination chemistry

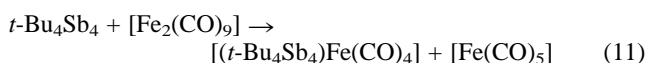
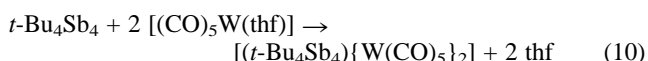
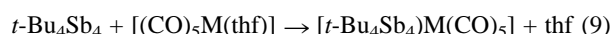
In order to investigate the use of *cyclo*-stibanes in coordination chemistry as antimony ligands, the four-membered ring *t*-

Bu<sub>4</sub>Sb<sub>4</sub> was chosen because it is an easily accessible, well defined starting material, soluble in hydrocarbons and stable at room temperature for a long time in absence of air and light.

Organoantimony rings generally have three types of reactive sites, which in combination open a broad spectrum of possible reactions leading to a variety of different structures. These sites are the lone pairs on the four antimony atoms, the antimony–carbon bonds and the antimony–antimony bonds. The known reactivity pattern of *t*-Bu<sub>4</sub>Sb<sub>4</sub> towards transition metal carbonyl complexes features all these possibilities. The antimony ring acts as mono or bidentate ligand through the lone pair of electrons. It is a precursor for transition metal substituted antimony rings which form with fission of the Sb–C bonds, and it is a source for 'naked' Sb<sub>*n*</sub> ligands, which implies fission and rearrangement of Sb–C and Sb–Sb bonds.

### 5.1 *t*-Bu<sub>4</sub>Sb<sub>4</sub> as a ligand in transition metal carbonyl complexes

The introduction of the intact *t*-Bu<sub>4</sub>Sb<sub>4</sub> molecule into the coordination sphere of transition metals requires relative mild conditions and soft reagents to avoid the decomposition of the ligand. These requirements are fulfilled in reactions with [M(CO)<sub>5</sub>(thf)] (M = Mo, W) or [Fe<sub>2</sub>(CO)<sub>9</sub>] in THF at room temperature and 1:1 or 1:2 complexes form, where the intact ring acts as monodentate or bidentate bridging ligand [eqn. (9)–(11)].<sup>11,12</sup> The reactivity of *t*-Bu<sub>4</sub>Sb<sub>4</sub> reflects the sterical hindrance of the complexation of the bulky ligand. The highest yield (90 %) is obtained for the iron complex, where the geometry of the ligand and the metal carbonyl moiety fit very well allowing a favourable staggered conformation along the Sb–Fe bond. The yields of the pentacarbonyl molybdenum and tungsten derivatives, where eclipsed conformations along the antimony metal bond cannot be avoided due to the C<sub>4v</sub> symmetry of the metal carbonyl group, are much lower, lying between 30 and 50%. The complexes formed are yellow crystalline solids, soluble in hydrocarbons. They are less air sensitive than the free antimony ring. Sometimes the bulky character of the ligand prevents reactions which proceed easily with less-bulky antimony ligands. No reaction occurs for instance between the norbornadiene complex [(nbd)Cr(CO)<sub>4</sub>] and *t*-Bu<sub>4</sub>Sb<sub>4</sub>, even under forcing conditions.



### 5.2 Structures of [(*t*-Bu<sub>4</sub>Sb<sub>4</sub>)Mo(CO)<sub>5</sub>], [(*t*-Bu<sub>4</sub>Sb<sub>4</sub>)W(CO)<sub>5</sub>]<sub>2</sub>, [(*t*-Bu<sub>4</sub>Sb<sub>4</sub>)Fe(CO)<sub>4</sub>], and [*t*-Bu<sub>3</sub>Sb<sub>4</sub>Mo(η<sup>5</sup>-C<sub>5</sub>Me<sub>5</sub>)(CO)<sub>3</sub>]

The structures of three complexes with the *t*-Bu<sub>4</sub>Sb<sub>4</sub> ligand and one complex with the *t*-Bu<sub>3</sub>Sb<sub>4</sub> ligand have been investigated by X-ray diffraction. The synthesis of the latter complex is shown in [eqn. (13)]. The molecular structures of the free ligand and of the complexes are depicted in Fig. 7. Selected geometric details are presented in Table 2.

The main features of the cyclic ligand are unaffected by the coordination of the metal carbonyl moieties. The antimony ring remains folded with the *t*-Bu substituents in the all-*trans* configuration. The inspection of the Sb–Sb–M and C–Sb–M angles (M = Mo, W, Fe) of [(*t*-Bu<sub>4</sub>Sb<sub>4</sub>)Mo(CO)<sub>5</sub>], [(*t*-Bu<sub>4</sub>Sb<sub>4</sub>)W(CO)<sub>5</sub>]<sub>2</sub>, and [(*t*-Bu<sub>4</sub>Sb<sub>4</sub>)Fe(CO)<sub>4</sub>] reveals that the metal carbonyl groups are inclined towards the periphery of the

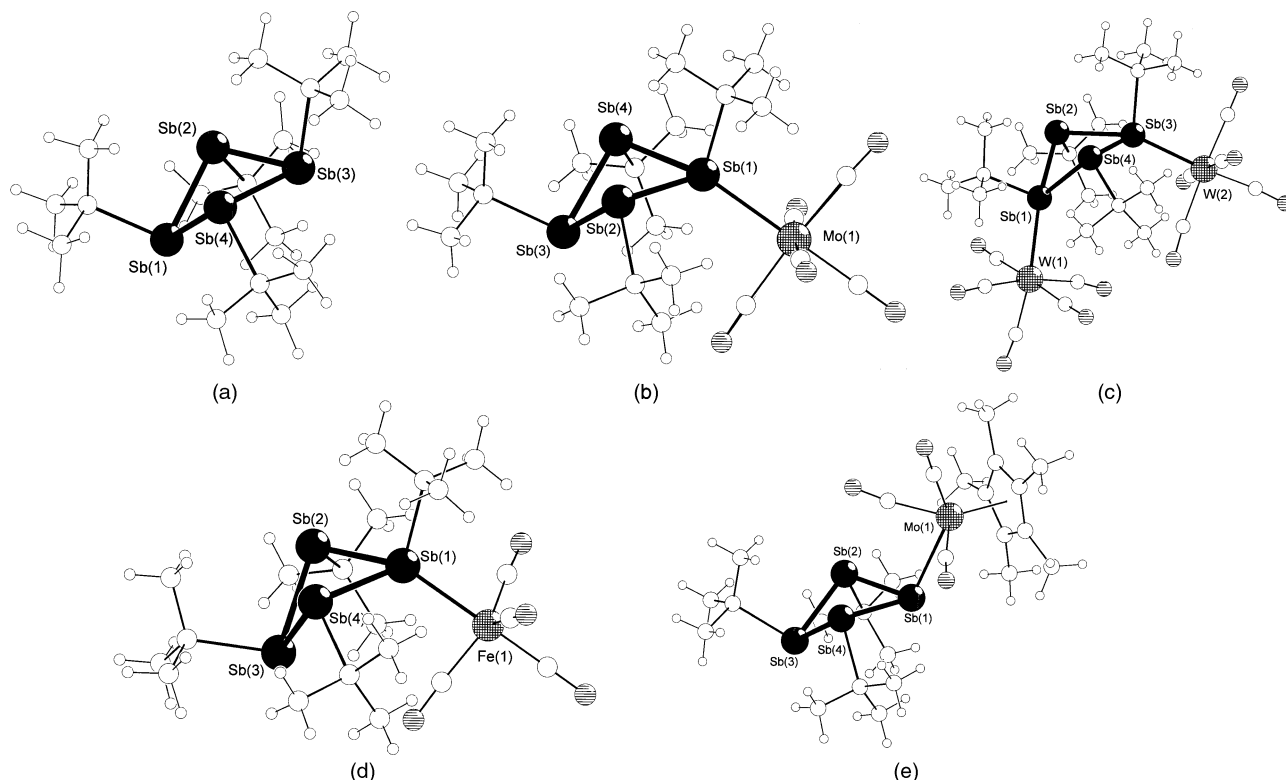


Fig. 7 Crystal structures of  $t\text{-Bu}_4\text{Sb}_4$ ,  $[(t\text{-Bu}_4\text{Sb}_4)\text{Mo}(\text{CO})_5]$ ,  $[(t\text{-Bu}_4\text{Sb}_4)\{\text{W}(\text{CO})_5\}_2]$ ,  $[(t\text{-Bu}_4\text{Sb}_4)\text{Fe}(\text{CO})_4]$ , and  $[(t\text{-Bu}_3\text{Sb}_4)\text{Mo}(\eta^5\text{-C}_5\text{Me}_5)(\text{CO})_3]$ .

Table 2 Selected bond lengths and angles of  $(t\text{-Bu}_4\text{Sb}_4)$  and complexes with  $t\text{-Bu}_n\text{Sb}_4$  ligands ( $n = 3, 4$ )

Compound	Sb–Sb/pm	Sb–M/pm	Sb–Sb–M/°	Fold angles/°	Ref.
$(t\text{-Bu}_4\text{Sb}_4)$	281.4(2)–282.1(2)			132.7, 132.8	13
$[(t\text{-Bu}_4\text{Sb}_4)\text{Mo}(\text{CO})_5]$	281.69(6)–283.74(6)	284.90(5)	127.71(2), 129.48(2)	123.3, 125.0	11
$[(t\text{-Bu}_4\text{Sb}_4)\text{Fe}(\text{CO})_4]$	281.78(5)–284.10(7)	254.22(8)	123.83(2), 123.95(2)	118.6, 119.2	11
$[(t\text{-Bu}_4\text{Sb}_4)\{\text{W}(\text{CO})_5\}_2]$	282.8(3)–285.1(3)	282.2(2), 284.7(3)	126.3(1)–134.5(1)	129.5, 130.0	12
$[(t\text{-Bu}_3\text{Sb}_4)\text{Mo}(\eta^5\text{-C}_5\text{Me}_5)(\text{CO})_3]$	281.45(5)–285.38(8)	288.39(6)	106.12(2), 107.30(2)	134.3, 134.4	11

antimony ring. The Sb–M bonds are longer than the corresponding values in sterically less strained complexes.<sup>11,12</sup>

A point of special interest is the influence of the coordination on the folding of the antimony ring (see Table 2). One might expect that the attachment of additional groups on the ring should lead to less folded systems. This should especially be true for  $[(t\text{-Bu}_4\text{Sb}_4)\{\text{W}(\text{CO})_5\}_2]$ , where the repulsion of the  $t\text{-Bu}$  groups in 1,3 positions should be compensated by the repulsive interactions of the  $\text{W}(\text{CO})_5$  groups. However, the fold angles are almost the same in the free ring and the dinuclear tungsten complex. In the case of the two 1:1 complexes the folding is even increased in comparison to the free ligand. A possible explanation could be that the metal carbonyl groups are pressed towards the neighbouring  $t\text{-Bu}$  groups and increase the repulsion between them. However, packing forces might also be responsible for the distortion of the antimony ring.

### 5.3 Reactions of $t\text{-Bu}_4\text{Sb}_4$ with $[(\eta^5\text{-Cp}^x)\text{Mo}(\text{CO})_3]_2$ ( $\text{Cp}^x = \text{C}_5\text{H}_5, \text{C}_5\text{Me}_5$ )

Reactions of  $t\text{-Bu}_4\text{Sb}_4$  with  $[(\eta^5\text{-Cp}^x)\text{Mo}(\text{CO})_3]_2$  ( $\text{Cp}^x = \text{C}_5\text{H}_5, \text{C}_5\text{Me}_5$ ) occur when the components are heated in refluxing toluene or decalin. Depending on the reaction conditions, different distributions of products are obtained resulting from the loss of CO from the molybdenum complex and the degradation of the antimony ring through loss of  $t\text{-Bu}$  groups as well as splitting and rearrangement of the Sb–Sb bonds. The conditions and the products are presented in the eqns. (12)–(14).<sup>14,15</sup>

These reactions demonstrate that in fact  $t\text{-Bu}_4\text{Sb}_4$  is a useful antimony source for complexes with the naked  $\text{Sb}_2$  and  $\text{Sb}_3$  ligands. The synthesis of  $[(\text{Cp}^x\text{Mo}(\text{CO})_2)_2\text{Sb}_2]$  has been achieved before using elemental (grey) antimony as reagent.<sup>16</sup> The yield of the  $\text{Sb}_2$  complex in this heterogeneous reaction was low however.

The complexes are well characterised by NMR and IR spectroscopy. The mass spectra of the  $\text{Sb}_2$  or  $\text{Sb}_3$  complexes are of particular interest. At low temperatures the molecular and fragment ions occur, proving the identity of the tetrahedrane complexes. At higher temperatures, however, the most abundant ions which occur at highest mass have the composition  $[\text{Cp}^x_2\text{Mo}_2\text{Sb}_5]^+$ . A section of mass spectra showing the signals with characteristic isotopic distribution is depicted in Fig. 8.

In view of these spectroscopic results it is remarkable that the neutral molecules of the composition  $[\text{Cp}^x_2\text{Mo}_2\text{Sb}_5]$  are not among the isolated products of reactions (12)–(14). Analogous complexes are well known in the coordination chemistry of  $\text{P}_5$  and  $\text{As}_5$  ligands. They are famous as triple decker complexes with planar  $\text{P}_5$  rings or  $\text{As}_5$  rings as the middle deck and form as the most stable species in the product mixtures when  $[\text{Cp}_2\text{Mo}_2(\text{CO})_6]$  is reacted with  $\text{P}_4$  or  $\text{As}_4$  until the evolution of CO is completed. There is little doubt that the ions observed in the gas phase are molecular ions of triple decker complexes with an  $\text{Sb}_5$  middle deck, resulting from rearrangement reactions of the  $\text{Sb}_2$  or *cyclo*- $\text{Sb}_3$  complexes under the conditions of mass spectrometry. A theoretical study showed that, due to Jahn–Teller distortion, an  $\text{Sb}_5$  ligand, if existent, would not have equal Sb–Sb bonds but would consist rather of two fragments,  $\text{Sb}_2$  and  $\text{Sb}_3$ .<sup>17</sup>

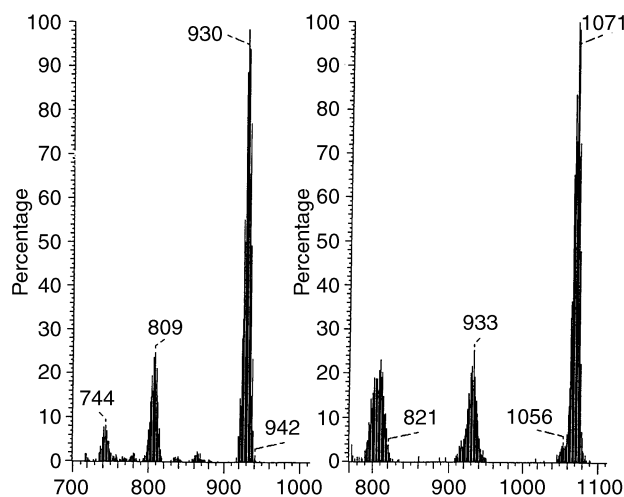
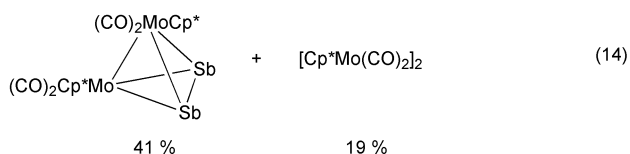
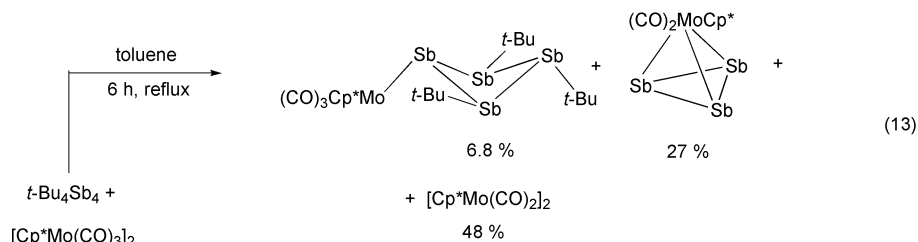
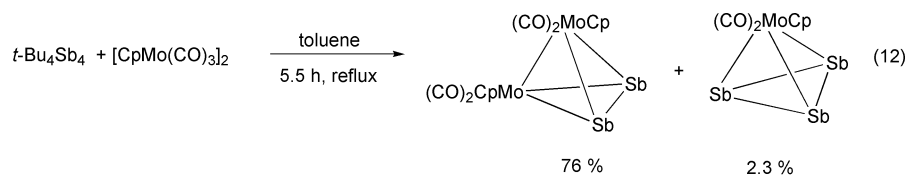


**Fig. 8** Mass spectra of the fragments  $[\text{Cp}^*_2\text{Mo}_2\text{Sb}_4]^+$  and  $[\text{Cp}^*_2\text{Mo}_2\text{Sb}_5]^+$  (left,  $\text{Cp}^x = \text{C}_5\text{H}_5$ ; right,  $\text{Cp}^x = \text{C}_5\text{Me}_5$ ).

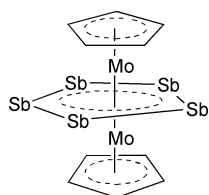


**Fig. 9** Probable structure of  $\text{Cp}^*_2\text{Mo}_2\text{Sb}_5$ .

What might be the reasons for the lower stability of  $[\text{Cp}^*_2\text{Mo}_2\text{Sb}_5]$  in condensed phases compared to analogous phosphorus or arsenic complexes? One possibility might be that the central  $\text{Sb}_5$  core is not sufficiently protected by the  $\text{Cp}^*\text{Mo}$  units and decomposition with formation of elemental antimony can occur. The dimensions of the planar  $\text{P}_5$  or  $\text{As}_5$  units are smaller and the tendency to rearrange with formation of the element are less expressed.

The structures of the tetrahedrane molecules  $[\text{CpMo}(\text{CO})_2\text{Sb}_3]$  and  $[\text{Cp}^*\text{Mo}(\text{CO})_2\text{Sb}_3]$  are depicted in Fig. 10. Selected distances and angles of the  $\text{Sb}_2$  and  $\text{Sb}_3$  complexes and of the anion of  $[\text{K}(\text{pmdeta})_2][t\text{-Bu}_4\text{Sb}_3]$  ( $\text{pmdeta} =$

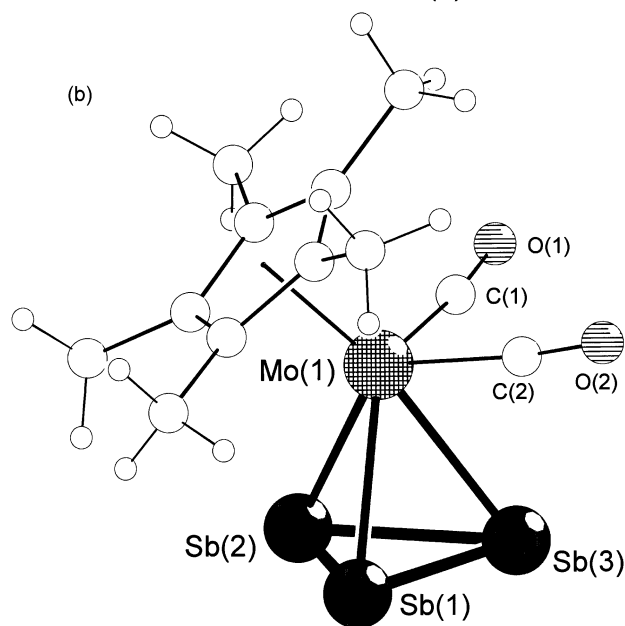
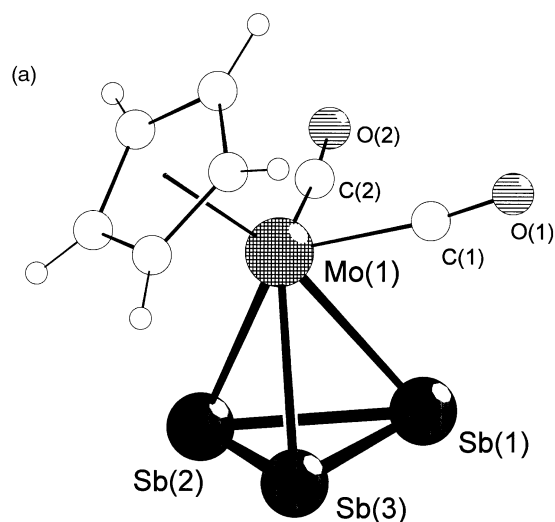


**Fig. 10** Molecular structures of  $[\text{CpMo}(\text{CO})_2\text{Sb}_3]$  and  $[\text{Cp}^*\text{Mo}(\text{CO})_2\text{Sb}_3]$ .

**Table 3** Geometric parameters for [Cp<sup>\*</sup>Mo(CO)<sub>2</sub>Sb<sub>3</sub>], [(CpMo(CO)<sub>2</sub>)<sub>2</sub>Sb<sub>2</sub>], and [Sb<sub>3</sub>(*t*-Bu)<sub>4</sub>]<sup>−</sup>

Compound	Sb–Sb/pm	Sb–Mo/pm	Ref.
[CpMo(CO) <sub>2</sub> Sb <sub>3</sub> ]	273.5(1)–278.1(1)	286.1(1)–294.9(1)	14, 15
[(CpMo(CO) <sub>2</sub> ) <sub>2</sub> Sb <sub>2</sub> ]	267.8(1)	276.2(1), 285.4(1)	16
[Cp <sup>*</sup> Mo(CO) <sub>2</sub> Sb <sub>3</sub> ]	273.97(9)–276.82(8)	285.12(8)–292.52(9)	14, 15
[Sb <sub>3</sub> ( <i>t</i> -Bu) <sub>4</sub> ] <sup>−</sup>	276.43(9), 276.69(7)	Sb–Sb–Sb: 86.23(3) <sup>o</sup>	18

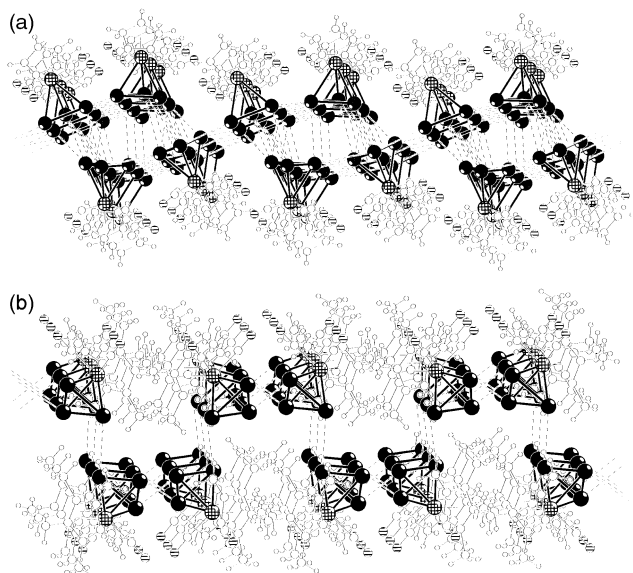


**Fig. 11** Arrangement of the [Cp<sup>\*</sup>Mo(CO)<sub>2</sub>Sb<sub>3</sub>] molecules in the crystal; (a), Cp<sup>\*</sup> = Cp, (b), Cp<sup>\*</sup> = Cp<sup>\*</sup>.

(Me<sub>2</sub>NCH<sub>2</sub>CH<sub>2</sub>)<sub>2</sub>NMe) are given in Table 3. The synthesis of this salt is described in eqn. (17).

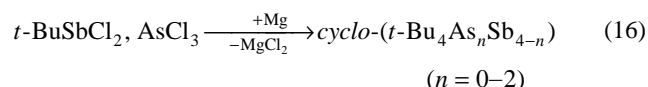
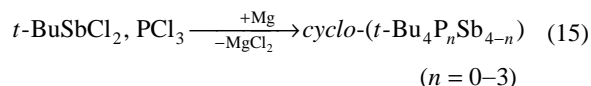
Interesting aspects of the structures of the Sb<sub>3</sub> complexes are the intermolecular contacts in the solid state (Fig. 11). The crystals consist of double layers of molecules which are connected through short intermolecular Sb⋯Sb contacts inside the layers. The Cp(CO)<sub>2</sub>Mo groups are directed into the space between the layers. The layers consist of wavy sheets of four molecules which overlap in a tile-like fashion. The layers of [Cp<sup>\*</sup>(CO)<sub>2</sub>MoSb<sub>3</sub>] are less compact due to the bulkiness of the Cp<sup>\*</sup> groups. They consist of transposed sheets of two molecules width. A section through the layers reveals the arrangement of the antimony atoms as rectangular meander. Close intermolecular Sb⋯Sb contacts are not unusual for molecules containing Sb–Sb bonds. They occur in distibanes Sb<sub>2</sub>R<sub>4</sub> or *cyclo*-stibanes when the antimony atoms are not protected by bulky substituents.<sup>1</sup> The electron delocalisation in chains or layers is responsible for bathochromic shifts that accompany the transition between the fluid state (isolated molecules) and the solid state (supramolecular aggregates). A good example of this behaviour is [Cp(CO)<sub>2</sub>MoSb<sub>3</sub>], which is yellow in solutions in hydrocarbons but dark red in the crystalline state.

An interesting feature of the Sb<sub>2</sub> and Sb<sub>3</sub> tetrahedranes is their relation to the Sb<sub>4</sub> molecules. This molecular form of the element antimony prevails in the gas phase but is unstable in the condensed phase where rearrangement occurs and the layers of metallic, grey antimony form. The Sb<sub>3</sub>Mo tetrahedranes are closely related to the Sb<sub>4</sub> molecules and it may be enlightening to consider the association of the MoSb<sub>3</sub> units as models of the first steps of the rearrangement process between the Sb<sub>4</sub>

molecules and the antimony layers of grey antimony which occurs when antimony vapour is condensed.

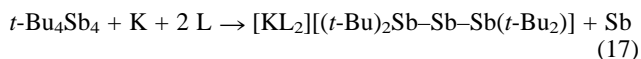
## 6 Sb, P and Sb, As heterocycles, the reaction of *t*-Bu<sub>4</sub>Sb<sub>4</sub> with K, and the structure of the *t*-Bu<sub>4</sub>Sb<sub>3</sub><sup>−</sup> ion<sup>18</sup>

The reaction of *t*-BuSbCl<sub>2</sub> and ECl<sub>3</sub> (E = P, As) with magnesium in boiling tetrahydrofuran leads to four-membered heterocycles *t*-Bu<sub>4</sub>E<sub>*n*</sub>Sb<sub>4−*n*</sub> (E = P, *n* = 0–3; E = As; *n* = 0–2) [eqns. (15) and (16)] instead of the expected heteropolycyclic systems. The migration of *tert*-butyl groups from antimony to phosphorus or arsenic with formation of *t*-BuPCL<sub>2</sub> or *t*-BuAsCl<sub>2</sub> takes place prior to the reduction.



The relative yields of the rings indicate a random distribution of the *tert*-butyl groups between Sb and P or As rather than a preference for specific rings. The heterocycles have been characterised in the product mixtures by mass spectrometry and <sup>1</sup>H NMR and <sup>31</sup>P NMR techniques. Attempts to isolate specific heterocycles with reasonable effort from the product mixture failed.

A useful starting material for specific syntheses of the four-membered heterocycles *t*-Bu<sub>4</sub>E<sub>*n*</sub>Sb<sub>4−*n*</sub> (E = P, As; *n* = 1) could be the dianionic, three-membered antimony chain [(*t*-Bu)Sb–(*t*-Bu)–Sb(*t*-Bu)]<sup>2−</sup>. In an attempt to produce this dianionic chain the reaction of *t*-Bu<sub>4</sub>Sb<sub>4</sub> with potassium in the presence of (Me<sub>2</sub>NCH<sub>2</sub>CH<sub>2</sub>)<sub>2</sub>NMe (pmdeta) was investigated. Instead of a dianionic species, the salt [K(pmdeta)<sub>2</sub>][*t*-Bu<sub>4</sub>Sb<sub>3</sub>] with a mono anionic bent Sb<sub>3</sub> chain bearing the *tert*-butyl groups in terminal positions forms [eqn. (17)]. It is apparent that in the course of the reduction, in addition to the ring opening, migrations of the *tert*-butyl groups must also have taken place. It should be noted that a similar anion, Ph<sub>2</sub>Sb–Sb–SbPh<sub>2</sub><sup>−</sup> is formed also in the reaction of Ph<sub>3</sub>Sb with Li.<sup>19</sup> These independent results suggest a chemical and structural preference for these bent Sb<sub>3</sub> anions protected by terminal organic groups.



The cation consists of a potassium ion coordinated by two tridentate amine ligands. The anion, although a potential donating ligand does not coordinate the cation. The structure of the anion, as obtained by X-ray crystallography, is presented in Fig. 12. Selected geometrical data are given in Table 3.

## 7 Concluding remarks

Due to the progress in the chemistry of organoantimony homocycles, the ring sizes 3, 4 and 6 are now well established with various examples characterised by crystal structure analyses. Five-membered rings have been characterised by <sup>1</sup>H NMR methods, but an example of a satisfactory crystal structure of a five-membered monocycle is still missing. The first examples of organoantimony polycycles have been characterised, but efficient synthetic pathways are still rare. The first attempts to use a *cyclo*-stibane as a reagent showed that *t*-Bu<sub>4</sub>Sb<sub>4</sub> is a useful starting material for various types of

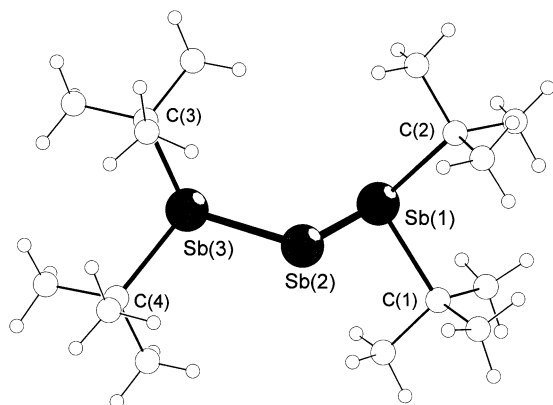


Fig. 12 Structure of the anion  $[t\text{-Bu}_4\text{Sb}_3]^-$ .

reactions including the formation of complexes with naked  $\text{Sb}_n$  ligands. However, despite this progress, the chemistry of antimony rings still has an exotic smell, and in fact special skills and experiences are useful in this field. This is especially true for the handling of the sterically less protected, more flexible antimony ring systems, which show the specific character of the  $\text{Sb}_n$  molecular skeleton more clearly. With bulky substituents such as  $(\text{Me}_3\text{Si})_2\text{CH}$  the antimony rings are effectively protected and resemble closely the analogous phosphorus or arsenic ring systems.

## 8 Acknowledgements

We thank the Deutsche Forschungsgemeinschaft and the Fonds der Chemischen Industrie for financial support. One of us (R. R.) thanks the Killam Trust for a Postdoctoral Fellowship.

## 9 References

- 1 H. J. Breunig and R. Rösler, *Coord. Chem. Rev.*, 1997, **163**, 33.
- 2 P. P. Power, *Chem. Rev.*, 1999, **99**, 3463.
- 3 H. Althaus, H. J. Breunig, R. Rösler and E. Lork, *Organometallics*, 1999, **18**, 328.
- 4 H. J. Breunig, W. Kanig and A. Soltani-Neshan, *Polyhedron*, 1983, **2**, 291.
- 5 H. J. Breunig, R. Rösler and E. Lork, *Angew. Chem.*, 1997, **109**, 2333; H. J. Breunig, R. Rösler and E. Lork, *Angew. Chem. Int., Ed. Engl.*, 1997, **36**, 2237.
- 6 H. J. Breunig, R. Rösler and E. Lork, *Organometallics*, 1998, **17**, 5594.
- 7 R. West, in *The Chemistry of Organic Silicon Compounds*, ed. S. Patai and Z. Rappoport, J. Wiley & Sons Ltd., Chichester, 1989, part 2, p. 1207.
- 8 H. J. Breunig, R. Rösler and E. Lork, *Angew. Chem.*, 1998, **110**, 3361; H. J. Breunig, R. Rösler and E. Lork, *Angew. Chem. Int. Ed. Engl.*, 1998, **37**, 3175.
- 9 M. Ates, H. J. Breunig, K. Ebert, S. Gülec, R. Kaller and M. Dräger, *Organometallics*, 1992, **11**, 145.
- 10 M. Baudler and K. Glinka, *Chem. Rev.*, 1993, **93**, 1623.
- 11 H. J. Breunig, R. Rösler and E. Lork, *Z. Anorg. Allg. Chem.*, 1999, **625**, 1619.
- 12 H. J. Breunig and J. Pawlik, *Z. Anorg. Allg. Chem.*, 1995, **621**, 817.
- 13 O. Mundt, G. Becker, H.-J. Wessely, H. J. Breunig and H. Kischkel, *Z. Anorg. Allg. Chem.*, 1982, **486**, 70.
- 14 H. J. Breunig, R. Rösler and E. Lork, *Angew. Chem.*, 1997, **109**, 2941; H. J. Breunig, R. Rösler and E. Lork, *Angew. Chem., Int. Ed. Engl.*, 1997, **36**, 2819.
- 15 R. Rösler, H. J. Breunig and E. Lork, *Phosphorus, Sulfur, Silicon Relat. Elem.*, 1997, **124 & 125**, 243.
- 16 J. R. Harper and A. L. Rheingold, *J. Organomet. Chem.*, 1990, **390**, C36.
- 17 W. Tremel, R. Hoffmann and M. Kertesz, *J. Am. Chem. Soc.*, 1989, **111**, 2030.
- 18 H. Althaus, H. J. Breunig, J. Probst, R. Rösler and E. Lork, *J. Organomet. Chem.*, 1999, **585**, 285.
- 19 R. A. Bartlett, H. V. Rasika Dias, H. Hope, B. D. Murray, M. M. Olmstead and P. P. Power, *J. Am. Chem. Soc.*, 1986, **108**, 6921.